

Supporting Information

Thermally insulated solar evaporator coupled with passive condenser for freshwater collection

Shuwen Cheng,^{‡a} Zhehao Sun,^{‡b} Yang Wu,^a Peng Gao,^a Jiaxin He^a, Zongyou Yin,^b

Liyong Liu^{*a} and Gang Li^{*c}

^aSchool of metallurgy, Northeastern University, Shenyang 100819, China.

^bResearch School of Chemistry, Australian National University, Canberra, ACT 2601, Australia.

^cDepartment of Chemical Engineering, The University of Melbourne, Melbourne, Victoria 3010, Australia.

[‡]These authors contributed equally to this work.

*Corresponding author

Email: liuly@smm.neu.edu.cn (Liyong Liu), li.g@unimelb.edu.au (Gang Li).

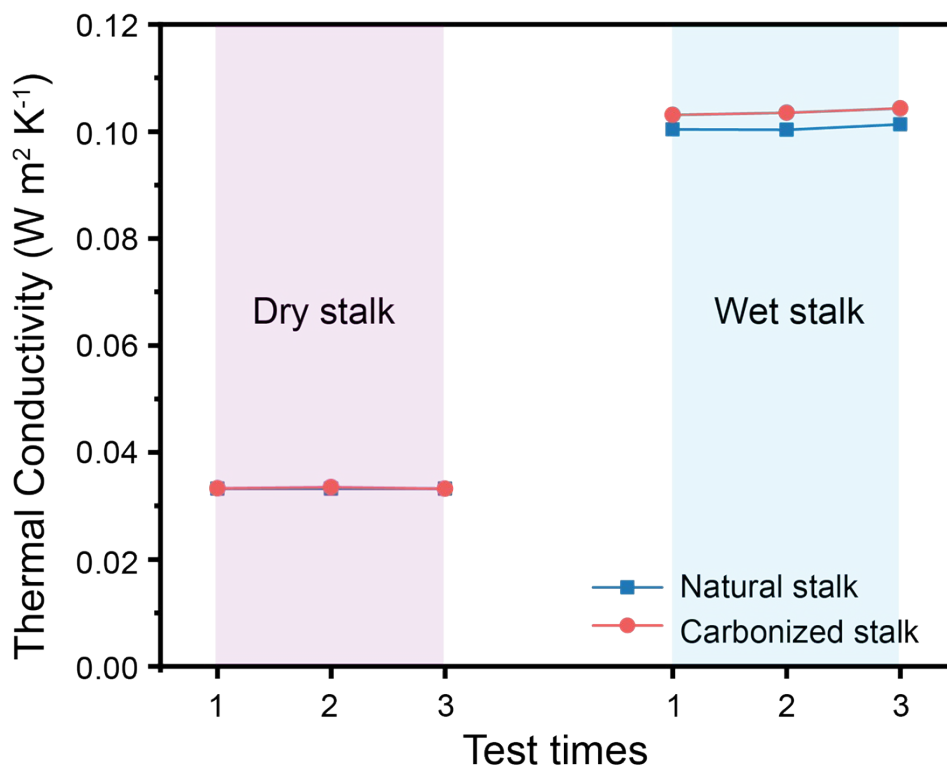


Figure S1. Measured thermal conductivities by hot-wire method under two experimental conditions (dry and wet).

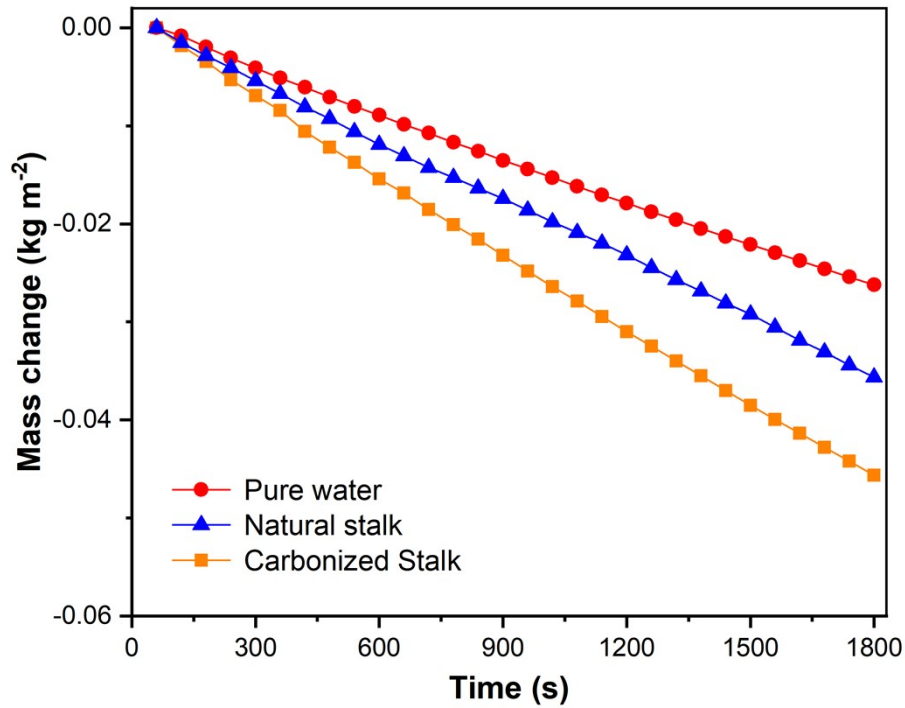


Figure S2. Mass change of water over time under dark condition ($C_{opt}=0$).

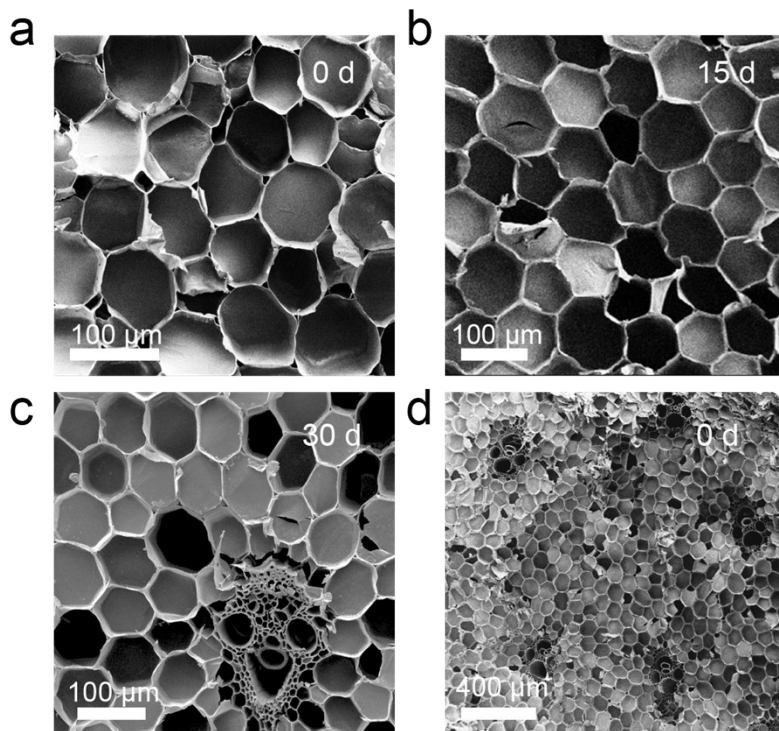


Figure S3. SEM images of natural stalk immersed in saltwater. (a) Immersed for 0 days: the top view of the tracheids' surface shows shapes of irregular hexagons. (b) Immersed for 15 days: the tracheid wall became more honeycomb-like with the increase of soaking time. (c) Immersed for 30 days: clear honeycomb tracheids and intact vascular bundles are shown. (d) Dense inner vascular bundles of reed stalk.

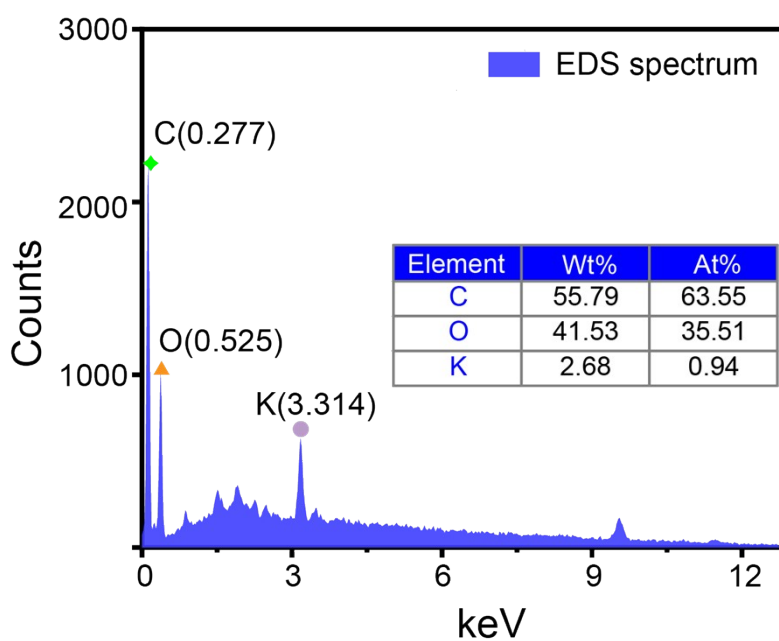


Figure S4. EDS spectrum of the natural reed stalk. Besides hydrogen, it is mainly composed of carbon, oxygen, and potassium, where potassium is a trace element, only 2.68wt%.

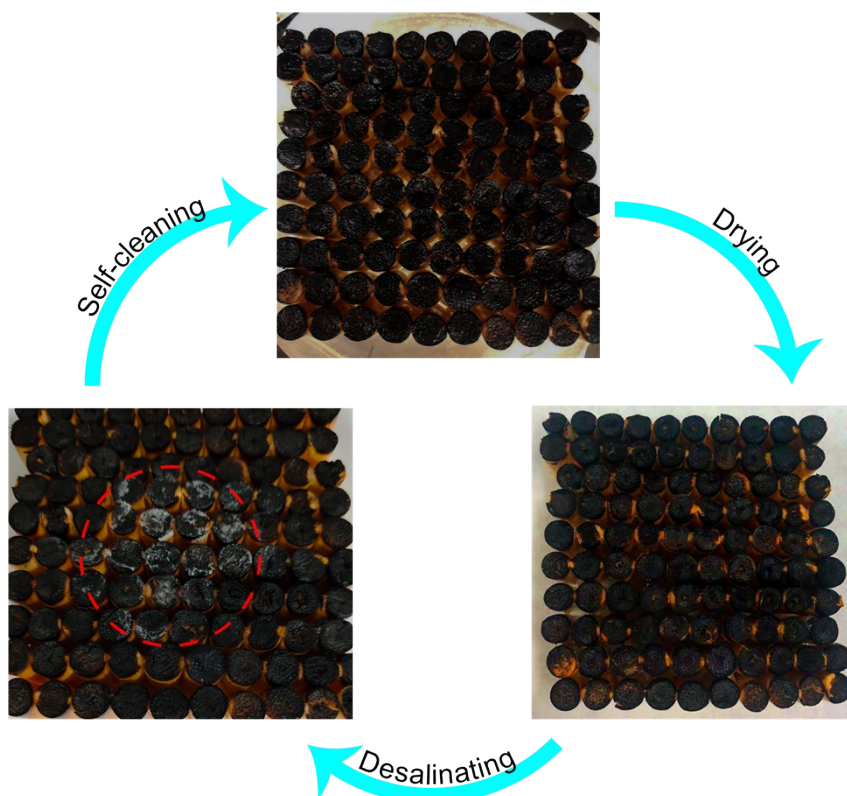


Figure S5. Images of the self-cleaning process (10×10 square array). Local salt deposition depends on the radiation radius of the light source.

Equation of solar-to-vapor efficiency¹:

$$\eta_{sv} = \frac{m_{net}(H_{LV} + C\Delta T)}{C_{opt}} \quad (S1)$$

$$H_{LV} = 1.91846 \times 10^3 \times \left[\frac{T_2}{T_2 - 33.91} \right]^2 \text{ kJ kg}^{-1} \quad (S2)$$

Where m_{net} is the net evaporation rate under solar illumination (the evaporation rate under dark condition was subtracted), H_{LV} represents the latent heat of water vaporization, C denotes the specific heat capacity of water (normally $4.2 \text{ kJ kg}^{-1} \text{ K}^{-1}$), ΔT is the temperature rise from the initial temperature T_1 to the maximum surface temperature T_2 , C_{opt} is the solar radiation power measured by an optical power meter (1000 W m^{-2} was used in this paper).

The analysis of heat loss:

The input heat flux is 1 kW m^{-2} , and five main strategies for energy consumption are as follows: (1) water evaporation, (2) reflection energy loss, (3) radiation heat loss, (4) convection heat loss, and (5) conductive heat loss.

(1) Water evaporation, η_w

The water evaporation consumption rate is equal to the evaporation efficiency; thus, η_w is **90.8%**.

(2) Reflection energy loss, $\eta_{ref,w}$

The solar absorption of a carbonized reed stalk is 96.8%; thus, the reflection loss $\eta_{ref,w}$ is **21%**.

(3) Radiation heat loss, $\eta_{rad,w}$

The radiation heat loss was calculated according to Stefan-Boltzmann Equation S3.

$$\Phi = \varepsilon A \sigma (T_1^4 - T_2^4) \quad (S3)$$

where Φ (W m^{-2}) is the radiation heat flux, A (m^2) is the surface area, σ is the Stefan-Boltzmann constant ($5.67 \times 10^{-8} \text{ W m}^{-2} \text{ K}^{-4}$), ε is the emissivity of material supposed as the maximum emissivity of 1 in this paper, T_1 (315.15 K) is the surface temperature of the carbonized reed stalk at steady state under 1 sun illumination, and T_2 (310.15 K) is the ambient temperature upward the material under 1 sun illumination. Therefore, according to equation (S3), the radiation heat flux is 34.6 W m^{-2} , which is $\sim 3.5\%$ of the solar flux Φ_0 (1 sun = 1000 W m^{-2}).

(4) Convection heat loss, $\eta_{conv,w}$

The convection heat flux was calculated by Newton's law of cooling:

$$Q_1 = hA\Delta T \quad (S4)$$

where Q_1 (W m^{-2}) is the convection heat flux, h ($10 \text{ W m}^{-2} \text{ K}^{-1}$) is the convection heat transfer coefficient, and ΔT is the different value between the surface temperature and the ambient temperature upward the material under 1 sun illumination ($\Delta T=5 \text{ K}$). According to Equation S5-S6, the convection heat flux is 40 W m^{-2} , which is $\sim 5\%$ of solar energy.

(5) Conduction heat loss, $\eta_{\text{cond,w}}$

The conduction heat flux was calculated according to the following Equation S5.

$$Q_2 = Cm\Delta T \quad (\text{S5})$$

where Q_2 is heat loss, C is the specific heat capacity of water ($4.2 \text{ J K}^{-1} \text{ g}^{-1}$), m (30 g) is the weight of water used in the paper, and ΔT (0.3 K) is the temperature difference of pure water after and before solar illumination under 1 sun after 1 h. According mentioned above, the conduction heat loss was calculated $\sim 20 \text{ W m}^{-2}$, which is $\sim 2\%$ of solar flux.

Table S1. Comparison of pore size of different biomass-derived materials.

Biomass-derived materials	Pore size (μm)
Sunflower ²	10-40
Sugarcane ³	20-100
Corn Straw ⁴	~1.5
Mushroom ⁵	~3.6
Lotus seedpod ⁶	0.016-1.46
Rice straw ⁷	5-20
This work	1-60

Table S2 Pore structure and porosity.

Pore area ($\text{m}^2 \text{g}^{-1}$)	Bulk density (g cm^{-3})	Apparent density (g cm^{-3})	Porosity %	Average pore diameter (μm)	Opened porosity %	Closed porosity %
41.07	0.0468	0.7579	93.83%	2	47.63%	46.20%

Movie S1. Capillary performance of reed stalk (removed the epidermis). This video highlights the superhydrophilicity of the carbonized reed stalk and ultrafast water transport in the stalk.

Movie S2. The superhydrophobic wax epidermis of reed stalk. This video highlights the superhydrophobic of the natural epidermis of reed stalk which can protect and ensure the salt tolerance in seawater.

Movie S3. The diffusion and convection traces of the concentrated brine from the surface of reed stalk evaporator arrays (RSEAs) to the brine underneath. This video intuitively embodies the self-cleaning performance of RSEAs.

References

1. P. Tao, G. Ni, C. Song, W. Shang, J. Wu, J. Zhu, G. Chen and T. Deng, *Nature Energy*, 2018, **3**, 1031-1041.
2. P. Sun, W. Zhang, I. Zada, Y. Zhang, J. Gu, Q. Liu, H. Su, D. Pantelic, B. Jelenkovic and D. Zhang, *ACS applied materials & interfaces*, 2019, **12**, 2171-2179.
3. J. Liu, Q. Liu, D. Ma, Y. Yuan, J. Yao, W. Zhang, H. Su, Y. Su, J. Gu and D. Zhang, *Journal of Materials Chemistry A*, 2019, **7**, 9034-9039.
4. Z. Sun, W. Li, W. Song, L. Zhang and Z. Wang, *Journal of Materials Chemistry A*, 2020, **8**, 349-357.
5. N. Xu, X. Hu, W. Xu, X. Li, L. Zhou, S. Zhu and J. Zhu, *Adv Mater*, 2017, **29**.
6. J. Fang, J. Liu, J. Gu, Q. Liu, W. Zhang, H. Su and D. Zhang, *Chemistry of Materials*, 2018, **30**, 6217-6221.
7. Q. Fang, T. Li, Z. Chen, H. Lin, P. Wang and F. Liu, *ACS applied materials & interfaces*, 2019, **11**, 10672-10679.